

1 This manuscript has been submitted to a peer-reviewed journal and is currently under  
2 review.

3

4

5 Manuscript Title: Integrating general and targeted biodiversity monitoring through  
6 parallel survey designs to improve indicator robustness

7

8 Authors: Francesc Sardà-Palomera<sup>1</sup>, Manel Puigcerver<sup>2</sup>, Irene Peña de la Cruz<sup>1,3</sup>, Marc  
9 Anton<sup>4</sup> & José Domingo Rodríguez-Teijeiro<sup>3</sup>

10

11 <sup>1</sup> Biodiversity Management and Conservation Program, Forest Science and Technology  
12 Center of Catalonia (CTFC), Solsona, Spain.

13 <sup>2</sup> Retired researcher, formerly at Universitat de Barcelona, Spain.

14 <sup>3</sup> IrBio and Departament de Biologia Evolutiva, Ecologia i Ciències Ambientals,  
15 Universitat de Barcelona, Spain.

16 <sup>4</sup>Catalan Ornithological Institute (ICO), Edifici Forum, Plaça Leonardo da Vinci 4-5,  
17 08019 Barcelona, Catalonia, Spain.

18

19 Corresponding author: Francesc Sardà-Palomera, e-mail: francesc.sarda@ctfc.cat

20

21 Keywords: biodiversity monitoring; calibration; detectability bias; long-term  
22 monitoring; species-specific surveys; volunteer-based monitoring; citizen science

23

24

25 **Abstract**

26 Breeding Bird Monitoring Schemes (BMS) provide large-scale, long-term data essential  
27 for biodiversity assessment and conservation decision-making. However, their  
28 multispecies design can generate species-specific detectability biases, particularly for  
29 taxa whose behavioral or ecological traits deviate from standardized count assumptions,  
30 potentially affecting abundance estimates and population indicators. We propose a  
31 structured integration framework linking general monitoring schemes with species-  
32 specific high-detection surveys through parallel designs and ecological modeling. The  
33 approach involves (1) implementing temporally matched general and targeted surveys,  
34 (2) modeling the relationship between survey outputs while incorporating ecological  
35 covariates influencing detectability differences, and (3) projecting the calibrated  
36 relationship onto broader BMS datasets to improve abundance indices and trend  
37 estimation.

38 We apply this framework to the Common Quail (*Coturnix coturnix*), a farmland game  
39 species with context-dependent detectability under standardized protocols. Parallel  
40 surveys revealed marked discrepancies between monitoring methods across habitat  
41 conditions. Incorporating habitat information into the calibration reduced detectability-  
42 related variability and improved the consistency of long-term trend estimates.

43 By formally linking general and targeted systems, this framework enhances the  
44 reliability and policy relevance of biodiversity indicators while retaining the spatial and  
45 temporal scalability of existing monitoring programs.

46

## 47 INTRODUCTION

48

49 Breeding bird monitoring schemes (BMS) are the cornerstone of large-scale biodiversity  
50 assessment worldwide (Gregory et al. 2005, Likens and Lindenmayer 2018). Their  
51 standardized protocols, broad spatial coverage and long-term continuity allow robust  
52 quantification of population change and ecological responses to environmental  
53 pressures through abundance-based indicators and trend indices (e.g.: Devictor et al.,  
54 2008; Rigal et al., 2023; Stephens et al., 2016). A defining feature of these schemes is  
55 their reliance on trained volunteer observers, whose coordinated effort generates large  
56 multispecies datasets that would be unfeasible through professional surveys alone  
57 (Moussy et al. 2022). By providing consistent information across extensive temporal  
58 and geographic scales, BMS programs play a key role in informing conservation policy,  
59 land-use planning and biodiversity indicators at national and international levels  
60 (Schmeller et al. 2009, Tulloch et al. 2013). Ensuring the methodological reliability and  
61 taxonomic representativeness of these schemes is therefore essential for accurately  
62 tracking environmental change (Yoccoz et al. 2001, Kissling et al. 2018).

63 Despite the success of BMS, their generalist and multispecies design inevitably  
64 introduces substantial variation in detection probability across species, habitats and  
65 regions (Thompson, W.L. 2002, Diefenbach et al. 2003). Species whose behavior,  
66 spatial dynamics or social organization depart from the assumptions of standard count  
67 protocols may yield biased indicators output in general monitoring schemes. Such  
68 biases may arise through missed detections, ambiguous records or potential double-  
69 counting (Guillera-Arroita et al. 2017). These issues are especially problematic for  
70 species that fall outside the core “common bird” set typically covered by BMS  
71 programs, including those that are behaviorally atypical, patchily distributed or  
72 otherwise difficult to survey using standard protocols (Nichols et al. 2007, Sardà-  
73 Palomera et al. 2012a).

74 Biases in detection probability can propagate through population indices, affecting  
75 abundance-based indicators, temporal trends and the ability of monitoring schemes to  
76 detect true demographic change (Kéry and Schmidt 2008). When detection is variable  
77 or inconsistent, yearly indices may become distorted, trend precision decreases and  
78 interannual variability inflates, particularly when uncertain observations are unevenly  
79 distributed across space or time (Johnson 2008, Kellner and Swihart 2014). In long-term

80 monitoring schemes, these effects can compromise the reliability and interpretability of  
81 populations.

82 As a consequence of these limitations, large-scale biodiversity indicators—such as those  
83 produced by the Pan-European Common Bird Monitoring Scheme (PECBMS, Brlík et  
84 al. 2021)—typically exclude species with low or highly variable detectability, focusing  
85 instead on widespread and consistently monitored taxa (Gregory et al. 2005, 2008, Brlík  
86 et al. 2021). This exclusion avoids introducing methodological noise into continental  
87 indicators, but it also means that many ecologically relevant or management-sensitive  
88 species remain poorly represented in general monitoring outputs. To address this gap,  
89 species-specific monitoring programs have been developed by universities, research  
90 institutes and public administrations, using tailored protocols that substantially increase  
91 detectability and provide more accurate abundance estimates for species whose behavior  
92 or ecology challenge standardized monitoring (Bibby et al. 2000).

93 Together, these challenges highlight the need not only for methodological comparisons  
94 between general BMS protocols and species-specific surveys (Johnson 2008), but for  
95 structured approaches that formally integrate information from both monitoring  
96 systems. Rather than treating general and targeted surveys as independent data streams,  
97 parallel implementations provide an opportunity to model systematic discrepancies and  
98 improve the robustness, consistency and comparability of abundance-based indicators  
99 derived from large-scale monitoring schemes (Kellner and Swihart 2014).

100 Here, we present a structured approach to integrate general and species-specific  
101 monitoring systems through parallel surveys and ecological modeling. We implement  
102 this approach by comparing indicator outputs from a general breeding bird monitoring  
103 scheme—the Catalan Common Bird Monitoring Survey (SOCC)— with those from a  
104 species-specific survey designed for the Common Quail (*Coturnix coturnix*), hereafter  
105 referred to as SEC, a farmland species whose behavioral and spatial dynamics generate  
106 highly variable detectability under standardized monitoring protocols. Using matched  
107 surveys, we (1) quantify differences in detection and abundance-based indicators  
108 between monitoring systems, (2) model how ecological conditions modulate these  
109 discrepancies, and (3) evaluate how integrating this information influences long-term  
110 population trend estimates. Through this case study, we illustrate how parallel survey

111 designs can strengthen the reliability and policy relevance of biodiversity indicators  
112 while retaining the spatial and temporal scalability of existing monitoring programs.

113

## 114 **DESCRIPTION OF THE MONITORING INTEGRATION APPROACH**

115

### 116 **Conceptual structure of the integration approach**

117

118 The integration approach presented here is based on the coordinated implementation  
119 of general multispecies monitoring protocols and species-specific high-detection  
120 surveys conducted under matched spatial and temporal conditions. The core premise is  
121 that systematic discrepancies between survey outputs contain information about  
122 context-dependent detection biases that can be explicitly modeled rather than treated  
123 as noise.

124

125 By structuring general and targeted monitoring as complementary components of a  
126 single analytical framework, differences in detection and abundance estimates can be  
127 quantified, related to ecological conditions, and projected onto larger monitoring  
128 datasets. This formal linkage improves indicator robustness while retaining the spatial  
129 and temporal scalability of existing monitoring infrastructures.

130

### 131 **Parallel survey design**

132 The proposed approach relies on the implementation of parallel surveys combining a  
133 general multispecies protocol with a species-specific high-detection survey carried out  
134 under comparable spatial and temporal conditions. Parallel sampling enables direct  
135 comparison of detection and count outputs while minimizing confounding effects of  
136 site, observer, and seasonal variation.

137

138 Surveys are conducted within the same localities and breeding period to ensure that  
139 observed discrepancies primarily reflect differences in protocol performance rather  
140 than temporal population change. When possible, synchronizing observer effort and

141 environmental conditions further reduces uncontrolled sources of variation.  
142 This paired design provides the empirical basis for modeling systematic differences  
143 between monitoring systems and underpins subsequent calibration and projection  
144 steps.

145

#### 146 [Modeling discrepancies between monitoring systems](#)

147 Parallel surveys provide paired observations from general and species-specific  
148 monitoring protocols, enabling quantitative assessment of discrepancies in detection  
149 and abundance estimates. Rather than assuming a constant proportional difference  
150 between survey outputs, the integration approach models their relationship explicitly,  
151 allowing for non-linear responses and context-dependent variation.

152 Ecological covariates that may influence detectability or survey performance can be  
153 incorporated into the modeling framework to account for environmental modulation of  
154 discrepancies. This step allows differences between monitoring systems to be  
155 interpreted as structured variation rather than random error.

156 By statistically relating counts from general monitoring schemes to those obtained  
157 under high-detection protocols, the approach generates a predictive relationship that  
158 can be applied to broader monitoring datasets. This modeling step forms the analytical  
159 core of the integration framework.

160

#### 161 [Projection to large-scale monitoring datasets](#)

162 Once the relationship between general and species-specific survey outputs has been  
163 modeled, the resulting predictive function can be applied to extended datasets  
164 generated by general monitoring schemes. This step allows discrepancies identified  
165 under paired sampling to be accounted for across wider spatial and temporal scales.

166 By adjusting general monitoring counts using the modeled relationship, abundance-  
167 based indicators and long-term trend estimates can be recalculated while explicitly  
168 incorporating context-dependent detectability differences. Because general monitoring  
169 programs typically provide longer time series and broader geographic coverage than

170 targeted surveys, this procedure enables improved inference without compromising  
171 continuity or scalability.

172 The projection stage thus links local calibration to large-scale indicator performance,  
173 completing the integration between general and specialized monitoring systems. To  
174 illustrate the implementation of this integration approach, we applied it to a case study  
175 focusing on the Common Quail.

176

## 177 **CASE STUDY: COMMON QUAIL**

178

### 179 **Study species**

180 The Common Quail is a small migratory galliform associated with open farmland in the  
181 Western Palearctic, particularly cereal crops and other herbaceous vegetation  
182 (McGowan et al. 2020). Individuals typically remain hidden within dense cover, making  
183 visual detection uncommon. Consequently, male vocalizations constitute the primary  
184 cue for detection in the field.

185 However, the environmental and social factors influencing calling activity remain  
186 poorly understood. Calling behavior is further shaped by a non-territorial mating  
187 system, characterized by loose and spatially dynamic male aggregations, whose calling  
188 intensity and spatial arrangement fluctuate in response to social interactions (Rodríguez-  
189 Teijeiro et al. 1992, Rodrigo-Rueda et al. 1997, Guyomarc'h et al. 1998, Sardà-  
190 Palomera et al. 2011). This behavioral complexity makes it difficult to predict when and  
191 where males will call, contributing to variable detectability across habitats and survey  
192 conditions.

193 In addition to these behavioral complexities, habitat quality strongly shapes the seasonal  
194 presence and abundance of the species. Quail distribution is known to shift in response  
195 to crop phenology and harvesting schedules, with individuals rapidly relocating as  
196 vegetation structure changes during spring and early summer (Rodríguez-Teijeiro et al.  
197 2009). Complementing this, remote-sensing analyses have shown that vegetation  
198 greenness (NDVI) provides a reliable proxy for these habitat dynamics, with higher  
199 NDVI values associated with increased quail presence (Sardà-Palomera et al. 2012b).

200 This combination of cryptic behavior, socially mediated calling patterns and strong  
201 dependence on dynamic habitat conditions poses major challenges for general bird  
202 monitoring schemes, where detectability-related biases directly affect indicator  
203 outputs. The species is also a widely harvested game bird across much of its range and  
204 has been subject to ongoing conservation concern, increasing the policy relevance of  
205 robust population indicators. In this context, inaccuracies linked to detectability bias  
206 may have direct implications for management decisions and stakeholder discussions.

207

## 208 [Monitoring schemes](#)

209

### 210 Common Bird Monitoring Survey (SOCC)

211

212 The Catalan Common Bird Monitoring Survey (SOCC, Herrando et al. 2008) is a  
213 volunteer-based scheme in which observers conduct standardized breeding bird counts  
214 along 3-km linear walking transects. Each transect is visited twice during the breeding  
215 season (15 April–15 May and 16 May–15 June), following a common protocol  
216 regarding survey duration (2–2.5 h), time of day (first four hours after sunrise), and  
217 weather conditions (no rain, low wind and good visibility). All individual birds  
218 (including Quails) detected by song or visually within the standardized survey period  
219 are recorded.

220 The SOCC program was established in 2002 and currently includes 638 transects across  
221 Catalonia. In this study, we used the subset of surveys conducted between 2005 and  
222 2025 in which the Common Quail was detected at least once ( $N = 205$  transects; Figure  
223 1). The starting year was selected because it coincides with the availability of spatially  
224 explicit agricultural land-use data, which allowed the identification of suitable habitat  
225 for subsequent analyses (see Section 2.3).

226

### 227 Common Quail Specific Survey (SEC)

228

229 The Common Quail Specific Survey (SEC; from its Catalan acronym) is a targeted  
230 monitoring protocol originally developed at the University of Barcelona to improve the

231 accuracy of quail counts based on behavioral research and extensive field experience  
232 with the species (Rodríguez-Teijeiro et al. 2010, Sardà-Palomera et al. 2012b). The  
233 method was designed to maximize the detection of singing males by accounting for  
234 their cryptic behavior, socially mediated calling activity and loose male aggregations.  
235 SEC surveys were conducted by trained professional personnel along predefined  
236 transects, following a structured sequence of listening stops and acoustic stimulation.

237 Observers moved along a fixed route and stopped at regular intervals to perform short  
238 listening sessions outside the vehicle. At each listening point, observers remained silent  
239 for 2 minutes to detect any spontaneously calling males. When spontaneous calling  
240 occurred, these males were immediately located and targeted for capture, as they  
241 provided reliable positional cues without requiring acoustic stimulation.

242 When no spontaneous calling was detected, observers broadcast female calls (“lure”) to  
243 stimulate vocal responses from males. The playback consisted of two series of 15–20  
244 seconds separated by short listening pauses. If males responded, their approximate  
245 locations were recorded and the observer attempted immediate capture using a hand net  
246 while continuing to use the playback device as the lure. If no response was elicited, the  
247 playback sequence was repeated 3 additional times (two series each), with 30-second  
248 listening intervals between repetitions.

249 At each listening point, this sequence allowed observers to: (1) activate males that were  
250 silent, (2) capture those that approached the lure, and (3) record those that continued  
251 calling but did not move toward the observer. While acoustic stimulation is intended to  
252 increase detectability and the number of males detected, capture aims to provide  
253 individual-level confirmation, allowing observers to discriminate between distinct  
254 individuals and to limit potential over-detection arising from moving individuals and  
255 repeated or socially mediated vocal responses. Captured males were held temporarily  
256 following ethical handling protocols.

257 At the end of the transect, all captured individuals were ringed and subsequently  
258 released at the precise point of capture. The final count for each transect consisted of the  
259 total number of males detected (captured + uncaptured), mapped at their initial detection  
260 position, with the aim of providing a high-detection reference of local abundance  
261 aligned with the behavioral characteristics of the species.

262

## 263 [Parallel sampling design](#)

264

265 Between 2021 and 2025, we designed and monitored 28 dedicated SOCC transects  
266 across Catalonia, spanning a wide range of quail suitable habitat types and altitudes  
267 (38–1158 m a.s.l.) and selected to represent areas where different quail densities were  
268 known or expected based on previous monitoring (Figure 1). Transects were  
269 progressively incorporated over the study period, resulting in variable annual sampling  
270 effort and partial overlap among years, with the maximum number of active transects  
271 reached in 2024 (n = 27). All surveys were carried out during the breeding season,  
272 between 1 April and 30 June. To ensure direct comparability between SOCC and SEC  
273 data, each transect was surveyed on two consecutive days: the SOCC survey was  
274 conducted first, followed the next day by the SEC survey at the same hour of the  
275 morning, under very similar weather conditions and by the same observer, and for the  
276 same duration. This standardized paired design minimized short-term temporal  
277 variation and ensured direct comparability between SOCC and SEC surveys under  
278 equivalent site, habitat, and weather conditions.

279

## 280 [Habitat and vegetation covariates](#)

281

282 To quantify the amount and quality of suitable breeding habitat available for Common  
283 Quails along each transect and season, we combined agricultural land-use information  
284 with remotely sensed vegetation indices. First, we identified the agricultural land-use  
285 categories considered suitable for the species based on previous studies and expert  
286 knowledge. These included cereal crops, fallows, legume crops, and herbaceous dryland  
287 mosaics, which represent the primary breeding habitats for the species in Mediterranean  
288 farmland systems. All polygons corresponding to these land-use categories were  
289 extracted from two official agricultural mapping systems: SIGPAC (the national land-  
290 parcel identification system) and DUN (the Catalan annual agricultural declaration  
291 system), both of which provide georeferenced information on crop types and field  
292 boundaries for each year between 2005 and 2025. A detailed description of the selected  
293 land-use categories is provided in Supporting Information.

294 For each 3-km transect and year, we quantified the amount of suitable habitat within a  
295 300-m buffer centered on the survey route. This buffer width was selected to match the  
296 effective detection distance used in the calibration analyses. All suitable habitat  
297 polygons intersecting the buffer were merged, and the resulting area was calculated for  
298 each transect–year combination. Suitable habitat area varied substantially among  
299 transects, ranging from 45 to 171 ha, and was included as a covariate in subsequent  
300 modelling steps.

301 To characterize vegetation productivity and structure, we extracted the Normalized  
302 Difference Vegetation Index (NDVI) for each transect buffer using Landsat surface  
303 reflectance imagery (Landsat 5, 7, 8, and 9; 30-m resolution). NDVI was calculated for  
304 each 15-day and monthly intervals between 1 April and 30 June of each year, following  
305 cloud and shadow masking based on the QA\_PIXEL band. For each interval, NDVI  
306 values were first aggregated at the pixel level using median composites, and transect-  
307 level NDVI was then obtained by spatially averaging (mean) all pixels contained within  
308 each buffered transect area. NDVI processing was conducted in Google Earth Engine  
309 (Gorelick et al. 2017). NDVI values derived from 15-day composites were unavailable  
310 for 16% of the paired surveys due to insufficient cloud-free observations, and these  
311 surveys were therefore excluded from analyses requiring habitat classification based on  
312 15-day NDVI. In contrast, monthly NDVI metrics were available for all surveys.

313 To classify SOCC transects into broad habitat-quality categories, we performed a k-  
314 means clustering analysis based on three NDVI descriptors calculated for each transect:  
315 the mean NDVI during the breeding season, the within-season standard deviation, and  
316 the interannual standard deviation (see Supporting Information). These metrics  
317 respectively captured overall vegetation greenness, short-term seasonal variability, and  
318 longer-term temporal stability. All variables were standardized prior to clustering. A  
319 two-cluster solution was selected based on minimization of the within-cluster sum of  
320 squares, yielding two distinct habitat-quality groups: transects characterized by high and  
321 stable vegetation greenness (high-quality habitat) and transects with lower and/or more  
322 variable NDVI values (low-quality habitat).

323

324 [Model implementation](#)

325

326 We developed a calibration model to relate SOCC counts to SEC counts using paired  
327 survey data. For each paired SOCC–SEC survey, the SEC count was used as the  
328 reference indicator of local abundance, and its relationship with the corresponding  
329 SOCC count was modelled using a generalized linear modelling framework. SOCC  
330 counts were included as the main predictor, and both linear and quadratic forms of the  
331 SOCC term were evaluated. Habitat covariates such as suitable-habitat area and NDVI  
332 were incorporated to account for local environmental variation, and interaction terms  
333 between SOCC and NDVI were also included among the candidate formulations.

334 To determine the most appropriate calibration structure, we fitted a full set of candidate  
335 models combining: (1) different NDVI metrics (mean, median, and monthly or 15-day  
336 composites), (2) alternative error distributions (Poisson, negative binomial NB1 and  
337 NB2), (3) the presence or absence of zero-inflation components, (4) linear versus  
338 quadratic SOCC effects and (5) models with or without a random intercept for transect  
339 identity. Candidate models were compared using Akaike’s Information Criterion (AIC),  
340 and the most parsimonious model structure was selected based on relative AIC  
341 differences. All models were inspected for residual patterns, dispersion, and potential  
342 outliers following standard diagnostic procedures. Final model performance was  
343 evaluated by assessing the agreement between predicted and observed SEC counts. In  
344 addition, the relative contribution of individual predictors was examined using  $\Delta$ AIC  
345 values derived from reduced models.

346 After selecting the final calibration model, SOCC counts from all transects where  
347 Common Quail had been detected at least once between 2005 and 2025 were converted  
348 into SEC-equivalent abundance indicators. For each transect and year, the observed  
349 SOCC count together with the corresponding habitat covariates was entered into the  
350 calibration model, and the resulting predictions were rounded down to the nearest  
351 integer to provide calibrated abundance-based indicators reflecting SEC-level  
352 detectability.

353

### 354 [Projection and trend estimation](#)

355

356 We assessed long-term population trends for both the original SOCC counts and the  
357 calibrated SEC-equivalent indicators. Annual SOCC and SEC-equivalent counts were

358 obtained by selecting, for each transect and year, the maximum value from the two  
359 SOCC visits, following the standard procedure used by the Catalan Institute of  
360 Ornithology (ICO) for deriving official SOCC trends.

361 For each dataset, we fitted TRIM log-linear models with site and time effects to estimate  
362 annual population indices and impute missing values (Van Strien et al. 2004). To obtain  
363 a single overall indicator trend, we regressed the logarithm of the TRIM-imputed annual  
364 index against time using ordinary least squares; the slope of this regression provided a  
365 measure of the average annual rate of change.

366 To evaluate whether trends differed across habitat quality, each transect was assigned to  
367 one of the NDVI-based habitat clusters (see Supporting Information), and the TRIM and  
368 log-linear trend analyses were repeated separately for each habitat group. Differences  
369 between the original SOCC and calibrated SEC-equivalent indices within each habitat  
370 group were formally tested using linear models in which the logarithm of the TRIM-  
371 derived annual index was modelled as a function of time (covariate), data series (SOCC  
372 vs calibrated SEC-equivalent; fixed factor), and their interaction. All analyses were  
373 conducted in R (version 4.4.2) using the rtrim package (Bogaart et al. 2020).

374

## 375 **RESULTS**

376

### 377 **Observed detection and count differences across schemes**

378

379 The paired SOCC–SEC surveys revealed clear differences in detectability between the  
380 two monitoring schemes. In 32% of paired surveys where SOCC recorded no Common  
381 Quails, the SEC protocol detected at least one calling male (mean  $\pm$  SD =  $4 \pm 3.4$ ),  
382 whereas the opposite pattern was rare, with SOCC detecting a single individual while  
383 SEC detected none in only one case (7%), corresponding to an isolated detection of a  
384 single calling male. Overall, presence–absence detections differed significantly between  
385 methods, with a clear asymmetry favoring SEC detections in surveys where SOCC  
386 failed (McNemar’s test,  $p = 0.033$ ).

387 Across all surveys, the SEC generally recorded higher numbers of calling males than  
388 the SOCC. In 71% of paired surveys, SEC detected more individuals than SOCC, while

389 26% yielded identical counts and only 3% (one case) resulted in higher counts under  
390 SOCC.

391 Consistently, SEC detected significantly more Common Quail males per survey than  
392 SOCC (paired Wilcoxon signed-rank test:  $p < 0.001$ ), with a mean difference of 3.5  
393 individuals per survey. On average, SOCC detected approximately 2.9 calling males per  
394 survey, whereas SEC detected approximately 6.4, corresponding to more than a twofold  
395 increase under the SEC protocol (Figure 2).

396

### 397 Calibration model performance

398

399 Model comparison showed that the best-performing calibration model was a negative-  
400 binomial formulation (NB1) including the 15-day mean NDVI together with linear and  
401 quadratic SOCC terms and  $\text{SOCC} \times \text{NDVI}$  interactions. Models using monthly NDVI  
402 metrics, or including random intercepts or zero-inflation components, all showed  
403 substantially higher AIC values.

404 The final calibration model (Table 1) captured a substantial proportion of the variability  
405 in SEC counts, providing a robust basis for converting SOCC-derived counts into SEC-  
406 equivalent abundance indicators (Supplementary material S3). Standard residual  
407 diagnostics indicated no relevant overdispersion, no zero inflation and no influential  
408 outliers, confirming robust model behavior.

409 An AIC-based assessment of predictor contributions revealed that NDVI was the most  
410 influential variable: removing NDVI together with its interactions produced by far the  
411 largest increase in AIC ( $\Delta\text{AIC} = 74.3$ ). The linear ( $\Delta\text{AIC} = 53.5$ ) and quadratic ( $\Delta\text{AIC} =$   
412  $20.0$ ) components of SOCC activity also contributed substantially to model fit,  
413 indicating a non-linear relationship between SOCC and SEC counts.  $\text{SOCC} \times \text{NDVI}$   
414 interactions further improved model performance ( $\Delta\text{AIC} = 8.9$ ), showing that the  
415 strength of the SOCC–SEC relationship varied along the NDVI gradient. In contrast,  
416 available habitat surface had no detectable effect ( $\Delta\text{AIC} = -1.9$ ). Overall, SEC counts  
417 were primarily driven by habitat greenness and SOCC activity, with NDVI modulating  
418 both the shape and magnitude of the calibration relationship.

419 The magnitude of the correction predicted by the calibration model varied across the  
420 SOCC–NDVI space. The largest discrepancies between SOCC and predicted SEC-  
421 equivalent indicators occurred when SOCC counts were low and NDVI values were  
422 high, whereas predicted SEC-equivalent counts and SOCC converged under conditions  
423 of low NDVI or when SOCC counts were relatively high ( $\geq 4$ ). These patterns reflect  
424 the structure of the fitted SOCC  $\times$  NDVI interactions (Figure 3).

425

## 426 Population trends

427

428 Applying the calibration model to the full SOCC dataset yielded SEC-equivalent  
429 abundance indicators for all transect–year combinations with available predictor  
430 information (N = 205 transects, 2005–2025).

431 TRIM analyses revealed minor differences in temporal patterns between the original  
432 SOCC counts and the calibrated SEC-equivalent indicator series. Across 2005–2025,  
433 the SOCC-based population index showed a slight decline ( $-2.1\%$  per year), whereas  
434 the calibrated series remained approximately stable ( $+0.1\%$  per year). A joint analysis of  
435 both series indicated that the difference in long-term trends was not statistically  
436 significant (time  $\times$  series:  $\beta = -0.028$ ,  $p = 0.066$ ), providing only weak evidence for  
437 divergence, and suggesting that, when all transects were pooled, both indices described  
438 broadly comparable overall trajectories (Figure 4A).

439 However, analyses stratified by NDVI-based habitat clusters revealed marked habitat-  
440 dependent differences. In transects characterized by habitat with high and stable NDVI  
441 values, the interaction between time and data series was statistically significant ( $\beta = -$   
442  $0.047$ ,  $p = 0.0079$ ). In these greener habitats, SOCC-based indices showed a clear  
443 decline ( $-4.51\%$  per year), whereas the calibrated SEC-equivalent indicator series  
444 remained stable ( $+0.15\%$  per year), indicating diverging temporal trajectories between  
445 the two approaches (Figure 4B).

446 In contrast, in transects with habitat with low or highly variable NDVI, the interaction  
447 was not statistically significant ( $\beta = -0.016$ ,  $p = 0.306$ ), and both SOCC and calibrated  
448 series produced similar long-term indicator trends (SOCC:  $-1.36\%$  per year; SEC-  
449 equivalent:  $+0.29\%$  per year). In these habitats, the two monitoring approaches yielded

450 broadly comparable temporal patterns, with limited divergence across the study period  
451 (Figure 4C).

452

## 453 **DISCUSSION**

454

455 Integrating general and species-specific monitoring systems provides a structured  
456 mechanism to address context-dependent detectability biases that can affect abundance-  
457 based indicators in multispecies monitoring schemes. Our results show that parallel  
458 survey designs allow systematic discrepancies between monitoring protocols to be  
459 quantified and modeled, improving the consistency and interpretability of indicator  
460 outputs.

461 The Common Quail represents a clear example of a broader class of species whose  
462 behavioral and ecological traits generate high variability in detectability across space  
463 and time (Thompson, W.L. 2002, Diefenbach et al. 2003, Guillera-Arroita et al. 2017).  
464 By incorporating a species-specific monitoring protocol and conducting parallel  
465 surveys, we quantified how these biological traits influence detection and indicator  
466 performance, and developed a habitat-informed calibration capable of reducing these  
467 discrepancies within a broad-scale monitoring framework.

468 Differences between the two methodologies were evident not only in abundance-based  
469 indicators but also in basic presence–absence detection, highlighting that detectability  
470 itself is a major source of divergence. Poor agreement in low-count situations suggests  
471 that many individuals remain undetected when spontaneous calling activity is low, a  
472 pattern common to species whose vocal behavior varies over short temporal scales  
473 (Bibby et al. 2000, Sutherland 2006). Under these conditions, passive multispecies  
474 surveys may fail to register a substantial fraction of individuals, whereas targeted  
475 protocols using acoustic stimulation can reveal a larger proportion of the population (De  
476 Rosa et al. 2022). This contrast illustrates how protocol-specific detection processes can  
477 generate systematic discrepancies in indicator outputs and underscores the value of  
478 explicitly modeling these differences within an integration framework.

479 NDVI emerged as the strongest environmental predictor in the calibration model,  
480 indicating that habitat greenness and phenological state strongly modulate discrepancies

481 between the two monitoring schemes. Importantly, the magnitude of the correction was  
482 not constant across sites: discrepancies were greatest in high-NDVI habitat when the  
483 BMS protocol recorded low counts. Because NDVI varies considerably among regions  
484 and years (Pettorelli et al. 2005), the degree of underestimation in BMS data is  
485 inherently context-dependent. Accordingly, the calibration does not act as a uniform  
486 multiplier but as a habitat-mediated adjustment shaped by local vegetation dynamics.  
487 On the other hand, the lack of a detectable effect of suitable-habitat area is consistent  
488 with the fact that all paired transects were located in landscapes where quails are  
489 normally present and habitat extent was not limiting. Within this range of conditions,  
490 habitat quality—as captured by NDVI—clearly outweighed habitat quantity in shaping  
491 differences between monitoring outputs.

492 Although the calibration improves the consistency of local abundance-based indicators,  
493 it is not designed to be directly extrapolated to derive absolute population sizes at  
494 regional or higher scales without accounting for population dynamics. In highly mobile  
495 species such as the Common Quail, males frequently undertake movements across  
496 farmland landscapes during the breeding season, tracking changes in vegetation  
497 structure, harvesting schedules and social cues (Puigcerver et al. 1989, Rodríguez-  
498 Teijeiro et al. 2009, Sardà-Palomera et al. 2012b). Recent GPS-based tracking data  
499 indicate that individuals may move not only between neighboring SOCC transects but  
500 also across wider regional, and occasionally international, distances within the same  
501 breeding period (Sardà-Palomera et al. 2025, unpublished data), highlighting the highly  
502 dynamic nature of populations over short temporal windows and the importance of  
503 interpreting calibrated counts within an explicitly defined spatial and temporal  
504 framework.

505 Such mobility implies open populations with substantial turnover, increasing the risk of  
506 double counting when survey data are aggregated across space and time without  
507 explicitly modelling movement and availability. Under these conditions, the local  
508 relationship between general and species-specific survey counts should be interpreted  
509 as a calibration of detectability rather than as a direct estimator of regional population  
510 totals. Nevertheless, this limitation does not preclude the use of calibrated counts for  
511 assessing temporal change or informing population indicators when embedded within

512 appropriate analytical frameworks that explicitly consider population openness and  
513 mobility.

514 Additional information on movement rates, seasonal redistribution, and connectivity  
515 among breeding areas will be essential to refine such models. In the long term,  
516 integrating movement data into calibration or state-space frameworks could allow more  
517 accurate estimates at larger spatial scales. For now, however, in highly mobile species,  
518 monitoring outputs should be interpreted within narrow temporal windows and, where  
519 appropriate, at ecologically meaningful spatial units (e.g., migratory flyways) rather  
520 than at lower administrative scales.

521 From a temporal perspective, the calibration refines the ability of general BMS data to  
522 describe long-term indicator trends. Although the uncorrected BMS series broadly  
523 captured the overall regional trajectory, the calibrated values reduced noise associated  
524 with detectability variability and produced indices that more closely reflect underlying  
525 temporal dynamics. This is particularly relevant for species whose detectability  
526 fluctuates within and across seasons. By stabilizing detection-related variability, the  
527 integration framework addresses a central concern in multispecies monitoring:  
528 detectability biases can propagate into long-term indices and compromise the ability of  
529 BMS programs to detect true demographic change (Kéry and Schmidt 2008, Kellner  
530 and Swihart 2014). Correcting these biases therefore enhances the reliability and  
531 interpretability of trend indicators.

532 Despite these limitations, BMS remain an indispensable component of large-scale  
533 biodiversity monitoring, providing unparalleled temporal and geographic coverage that  
534 no species-specific program could realistically achieve. The challenge, therefore, is not  
535 to replace general monitoring schemes, but to complement them through structured  
536 integration approaches that explicitly address detectability-related bias.

537 Methodologically, the proposed integration framework establishes a functional bridge  
538 between general and species-specific monitoring schemes. It leverages the extensive  
539 spatial and temporal coverage of BMS programs while embedding information from  
540 targeted surveys that maximize detectability. This integration allows general schemes to  
541 retain their logistical advantages without inheriting the full extent of their detectability  
542 biases. Beyond the present case, similar bridging approaches could be explored for other

543 species facing detectability challenges that require specialized monitoring protocols  
544 (e.g., *Crex crex*, *Burhinus oedicephalus*). In several taxa, dedicated monitoring programs  
545 now incorporate passive acoustic recorders (Sugai, et al. 2018), thermal-imaging  
546 devices (Lahoz-Monfortand Magrath, 2021) or camera-trap systems (Wearn and Glover-  
547 Kapfer 2019), among others, to increase detection rates under conditions where standard  
548 BMS protocols perform poorly. Although these technologies are generally too costly or  
549 labor-intensive for broad implementation within BMS networks, they can provide high-  
550 quality reference data that enable calibration or validation of general monitoring outputs  
551 in a manner analogous to the approach demonstrated here. Such complementary use of  
552 broad-scale and species-specific data provides a practical pathway to improve indicator  
553 robustness for species that are poorly sampled by standard monitoring schemes, while  
554 underscoring the ongoing challenge of translating detection-based information into  
555 reliable abundance-based indicators for long-term trend assessment.

556 Overall, our study demonstrates that general BMS data can be partially reconciled with  
557 species-specific information to improve abundance-based indicators and trend  
558 interpretation for species with highly variable detectability. By developing a calibration  
559 approach grounded in paired surveys and ecological context, we provide a practical  
560 framework that addresses major sources of detectability-related bias while retaining  
561 the extensive spatial and temporal coverage of general monitoring programs. However,  
562 the relationship estimated here is necessarily context-dependent. Behavioral patterns,  
563 population dynamics, and habitat phenology may vary across regions, years, or  
564 management systems, potentially altering the relationship between general and  
565 species-specific surveys. Consequently, applying this approach elsewhere may require  
566 region-specific calibration analyses to identify the most appropriate model structure.  
567 Despite this, the proposed framework offers a transferable methodological basis for  
568 integrating general and specialized monitoring schemes. More broadly, our results  
569 highlight the value of combining broad-scale volunteer-based programs with targeted  
570 high-detection surveys to generate more robust, interpretable, and policy-relevant  
571 population indicators for species whose detectability is shaped by behavioral or  
572 environmental processes.

573

574 **PERSPECTIVES AND APPLICATIONS**

575 Breeding bird monitoring schemes underpin many biodiversity indicators used in  
576 conservation policy and environmental reporting. However, species whose behavioral or  
577 ecological traits deviate from the assumptions of standardized multispecies protocols  
578 may be excluded from indicator frameworks or may generate biased abundance-based  
579 estimates. The integration approach presented here provides a structured way to  
580 diagnose and quantify such discrepancies by combining a general monitoring scheme  
581 with species-specific high-detection survey conducted under parallel sampling design.

582 Three main applied benefits arise from this approach. First, by explicitly modeling  
583 systematic differences between monitoring systems, the method allows detectability-  
584 related bias to be distinguished from random variation, increasing confidence in the  
585 interpretation of population indices. Second, once calibrated, the relationship between  
586 general and targeted surveys can be projected onto broader datasets, enabling long-term  
587 trend estimation that retains the spatial and temporal coverage of large-scale monitoring  
588 programs. Third, information gained from parallel surveys can inform future monitoring  
589 design, identifying ecological contexts in which general protocols are likely to  
590 underperform and guiding the strategic deployment of targeted surveys.

591 Although demonstrated here using a farmland game bird with context-dependent vocal  
592 behavior, the approach is applicable to other taxa for which detectability varies strongly  
593 across habitats, seasons, or behavioral states. Targeted surveys incorporating acoustic  
594 stimulation, passive acoustic recorders, thermal imaging, or other high-detection  
595 technologies can serve as reference systems for calibrating general monitoring outputs.  
596 In this way, broad-scale volunteer-based schemes can be complemented—not  
597 replaced—by strategically implemented specialized surveys.

598 By linking general and targeted monitoring through explicit calibration, this approach  
599 enhances the robustness and policy relevance of biodiversity indicators while  
600 preserving the logistical feasibility and long-term continuity of existing monitoring  
601 infrastructures. As biodiversity reporting frameworks and management policies  
602 increasingly rely on standardized indicators, integrating complementary monitoring  
603 systems offers a practical pathway to improve inference for species that would  
604 otherwise remain poorly represented.

605 **ACKNOWLEDGEMENTS**

606 We thank the Institut Català d'Ornitologia (ICO) for providing access to SOCC data and  
607 for its long-term commitment to bird monitoring in Catalonia. We are especially grateful  
608 to the volunteer observers, as well as to the students and field assistants who contributed  
609 to data collection and field logistics. This study was funded by the Subdirecció General  
610 de Fauna Cinegètica, Caça i Pesca Continental of the Departament d'Agricultura,  
611 Ramaderia, Pesca i Alimentació (Generalitat de Catalunya). Long-term monitoring  
612 through the SOCC program is supported by the Departament de Territori of the  
613 Generalitat de Catalunya.

614

615 **CONFLICT OF INTEREST STATEMENT**

616 The authors declare no conflicts of interest.

617

618 **DATA AVAILABILITY STATEMENT**

619 Data and code required to reproduce the analyses presented in this study are available  
620 via a private Zenodo repository for peer review at:

621 [626 The repository will be made publicly available and archived with a DOI upon  
627 acceptance of the manuscript.](https://zenodo.org/records/18773685?token=eyJhbGciOiJIUzUxMiJ9.eyJpZCI6IjE2YzMz<br/>622 MjA1LTlkZjEtNDJjZS1iMTNmLWMyODc3NjExNzMxNSIsImRhdGEiOiJ9LCJyZW5kb20iOiI<br/>623 3NGQzZDg5ZmFmZjVmZWwM2M2ZjI1MWEyMDYwOGU2ZCJ9.4mhJdHo-<br/>624 cnr950p70RTAqNgO8GQd5el330_YDf4Uun57Mekaikt9dOlenawysKv0y_QOx1elp9aPTE<br/>625 NgHQ6s0w.</a></p></div><div data-bbox=)

628

629 **REFERENCES**

630 Arroyo, B., M. Fernández-Tizón, and F. Sardà-Palomera. 2022. Análisis de los datos del  
631 programa SACRE relativos a la codorniz común (*Coturnix coturnix*) en la España  
632 Peninsular. IREC-CTFC.

633 Bibby, C. J., N. D. Burgess, and Hill, D.A. 2000. Bird census techniques. Elsevier.

634 Bogaart, P., M. van der Loo, J. Pannekoek, and M. P. Bogaart. 2020. Package 'rtrim.'

635 Trends and Indices for Monitoring Data.

636 Brlík, V., E. Šílarová, J. Škorpilová, H. Alonso, M. Anton, A. Aunins, Z. Benkő, G. Biver, M.

637 Busch, and T. Chodkiewicz. 2021. Long-term and large-scale multispecies

638 dataset tracking population changes of common European breeding birds.

639 Scientific data 8:21.

640 De Rosa, A, Castro, I., and Marsland, S. 2022. The acoustic playback technique in avian

641 fieldwork contexts: a systematic review and recommendations for best practice.

642 Ibis 164.

643 Devictor, V., R. Julliard, D. Couvet, and F. Jiguet. 2008. Birds are tracking climate

644 warming, but not fast enough. Proceedings. Biological sciences / The Royal

645 Society 275:2743–8.

646 Diefenbach, D. R., D. W. Brauning, and J. A. Mattice. 2003. Variability in grassland bird

647 counts related to observer differences and species detection rates. The Auk

648 120:1168–1179.

649 Escandell, V., S. Herrando, and S. Escudero. 2023. Tendencia de las aves en primavera.

650 Pages 78–81 SEO/BirdLife. Programas de seguimiento y grupos de trabajo de

651 SEO/BirdLife 2023. SEO/BirdLife. Madrid.

652 Gorelick, N., M. Hancher, M. Dixon, S. Ilyushchenko, D. Thau, and R. Moore. 2017.

653 Google Earth Engine: Planetary-scale geospatial analysis for everyone. Remote

654 sensing of Environment 202:18–27.

655 Gregory, R. D., A. van Strien, P. Vorisek, A. W. Gmelig Meyling, D. G. Noble, R. P. B.

656 Foppen, and D. W. Gibbons. 2005. Developing indicators for European birds.

657 Philosophical transactions of the Royal Society of London. Series B, Biological  
658 sciences 360:269–288.

659 Gregory, R. D., P. Voříšek, D. G. Noble, A. Van Strien, A. Klvaňová, M. Eaton, A. W.  
660 Gmelig Meyling, A. Joys, R. P. B. Foppen, and I. J. Burfield. 2008. The generation  
661 and use of bird population indicators in Europe. *Bird Conservation International*  
662 18.

663 Guillera-Aroita, G., J. J. Lahoz-Monfort, A. R. van Rooyen, A. R. Weeks, and R. Tingley.  
664 2017. Dealing with false-positive and false-negative errors about species  
665 occurrence at multiple levels. *Methods in Ecology and Evolution* 8:1081–1091.

666 Guyomarc’h, J. C., O. Combreau, M. Puigcerver, P. A. Fontoura, and N. J. Aebischer.  
667 1998. Quail. Page BWP Update 2. Oxford University Press, Oxford.

668 Herrando, S., L. Brotons, J. Estrada, and V. Pedrocchi. 2008. The Catalan Common Bird  
669 Survey ( SOCC ): a tool to estimate species population numbers:138–146.

670 ICO. 2025. Vint-i-tresè informe del Programa de Seguiment d’Ocells Comuns a  
671 Catalunya (SOCC). Institut Català d’Ornitologia (IC).

672 Johnson, D. H. 2008. In defense of indices: the case of bird surveys. *The Journal of*  
673 *Wildlife Management* 72:857–868.

674 Kellner, K. F., and R. K. Swihart. 2014. Accounting for imperfect detection in ecology: a  
675 quantitative review. *PloS one* 9:e111436.

676 Kéry, M., and B. Schmidt. 2008. Imperfect detection and its consequences for  
677 monitoring for conservation. *Community Ecology* 9:207–216.

678 Kissling, W. D., J. A. Ahumada, A. Bowser, M. Fernandez, N. Fernández, E. A. García, R. P.  
679 Guralnick, N. J. Isaac, S. Kelling, and W. Los. 2018. Building essential biodiversity

680 variables (EBV s) of species distribution and abundance at a global scale.  
681 Biological reviews 93:600–625.

682 Lahoz-Monfort, J.J., and Magrath, M.J.L. 2021. A comprehensive overview of  
683 technologies for species and habitat monitoring and conservation. *BioScience*  
684 71:1038-1062.

685 Likens, G., and D. Lindenmayer. 2018. *Effective ecological monitoring*. CSIRO publishing.

686 McGowan, P., G. Kirwan, E. de Juana, and P. Boesman. 2020. Common quail (*Coturnix*  
687 *coturnix*), version 1.0. *Birds of the World*.

688 Moussy, C., I. J. Burfield, P. J. Stephens, Newton, A.F.E, S. H. M. Butchart, W. Sutherland,  
689 R. D. Gregory, McRae, Louise, Bubb, P., Roesler, I., Ursino, C., Wu, Y., Retief, E.F.,  
690 Udin, J.S., Urazaliyev, R., Sánchez-Clavijo, L.M., Lartey, E., and Donal, P.F. 2022.  
691 A quantitative global review of species population monitoring. *Conservation*  
692 *Biology* 36.

693 Nichols, J. D., J. E. Hines, D. I. Mackenzie, M. E. Seamans, and R. J. Gutierrez. 2007.  
694 Occupancy estimation and modeling with multiple states and state uncertainty.  
695 *Ecology* 88:1395–1400.

696 Perennou, C., C. 2009. European Union Management Plan Common quail. Page 71.  
697 European Commission.

698 Pettorelli, N., J. O. Vik, A. Mysterud, J.-M. Gaillard, C. J. Tucker, and N. C. Stenseth. 2005.  
699 Using the satellite-derived NDVI to assess ecological responses to  
700 environmental change. *Trends in ecology & evolution* 20:503–10.

701 Puigcerver, M., J. D. Rodríguez-Teijeiro, and S. Gallego. 1989. Migración y/o nomadismo  
702 en la codorniz (*Coturnix c. coturnix*)? *Etologia* 1:39–45.

703 Rigal, S., V. Dakos, H. Alonso, A. Auniņš, Z. Benkő, L. Brotons, T. Chodkiewicz, P.  
704 Chylarecki, E. De Carli, and J. C. Del Moral. 2023. Farmland practices are driving  
705 bird population decline across Europe. *Proceedings of the National Academy of*  
706 *Sciences* 120:e2216573120.

707 Rodrigo-Rueda, F. J., J. D. Rodríguez-Teijeiro, M. Puigerver, and S. Gallego. 1997. Mate  
708 switching in a non-monogamous species? The case of the common quail  
709 (*Coturnix coturnix*). *Ethology* 103:355–364.

710 Rodríguez-Teijeiro, J. D., M. Puigerver, and S. Gallego. 1992. Mating strategy in the  
711 European Quail (*Coturnix c. coturnix*) revealed by male population density and  
712 sex-ratio in Catalonia (Spain). *Gibier faune sauvage* 9:377–386.

713 Rodríguez-Teijeiro, J. D., F. Sardà-Palomera, I. Alves, Y. Bay, A. Beça, B. Blanchy, B.  
714 Borgogne, B. Bourgeon, P. Colaço, J. Gleize, A. Guerreiro, M. Maghnoij, C.  
715 Rieutort, D. Roux, and M. Puigerver. 2010. Monitoring and management of  
716 common quail *coturnix coturnix* populations in their atlantic distribution area.  
717 *Ardeola* 57:135–144.

718 Rodríguez-Teijeiro, J. D., F. Sardà-Palomera, J. Nadal, X. Ferrer, C. Ponz, and M.  
719 Puigerver. 2009. The effects of mowing and agricultural landscape  
720 management on population movements of the common quail. *Journal of*  
721 *Biogeography* 36:1891–1898.

722 Sardà-Palomera, F., L. Brotons, D. Villero, H. Sierdsema, S. E. Newson, and F. Jiguet.  
723 2012a. Mapping from heterogeneous biodiversity monitoring data sources.  
724 *Biodiversity and Conservation* 21:2927–2948.

725 Sardà-Palomera, F., M. Puigcerver, L. Brotons, and J. D. Rodríguez-Teijeiro. 2012b.

726 Modelling seasonal changes in the distribution of Common Quail *Coturnix*

727 *coturnix* in farmland landscapes using remote sensing. *Ibis* 154:703–713.

728 Sardà-Palomera, F., M. Puigcerver, D. Vinyoles, and J. D. D. Rodríguez-Teijeiro. 2011.

729 Exploring male and female preferences, male body condition, and pair bonds in

730 the evolution of male sexual aggregation: the case of the Common Quail (

731 *Coturnix coturnix* ). *Canadian Journal of Zoology* 89:325–333.

732 Sardà-Palomera, M. Puigcerver, Moreno-Zarate, L., Santisteban, C., and Rodríguez-

733 Teijeiro, J.D. 2025. First quail (*Coturnix coturnix*) markings with GPS confirm

734 previous knowledge and provide new key information for its conservation.

735 Valencia.

736 Schmeller, D. S., P.-Y. Henry, R. Julliard, B. Gruber, J. Clobert, F. Dziock, S. Lengyel, P.

737 Nowicki, E. Déri, E. Budrys, T. Kull, K. Tali, B. Bauch, J. Settele, C. Van Swaay, A.

738 Kobler, V. Babij, E. Papastergiadou, and K. Henle. 2009. Advantages of

739 volunteer-based biodiversity monitoring in Europe. *Conservation biology : the*

740 *journal of the Society for Conservation Biology* 23:307–16.

741 Stephens, P. A., L. R. Mason, R. E. Green, R. D. Gregory, J. R. Sauer, J. Alison, A. Aunins,

742 L. Brotons, S. H. Butchart, and T. Campedelli. 2016. Consistent response of bird

743 populations to climate change on two continents. *Science* 352:84–87.

744 Sugai, L. S. M., Silva, T. S. F., Ribeiro, J. W., and Llusia, D. 2018. Terrestrial Passive

745 Acoustic Monitoring: Review and Perspectives. *BioScience*:15–25.

746 Sutherland, W. J. 2006. *Ecological census techniques: a handbook*. Cambridge

747 university press.

748 Thompson, W.L. 2002. Towards reliable bird surveys: accounting for individuals present  
749 but not detected. *The Auk* 119:18–25.

750 Tulloch, A. I., H. P. Possingham, L. N. Joseph, J. Szabo, and T. G. Martin. 2013. Realising  
751 the full potential of citizen science monitoring programs. *Biological*  
752 *Conservation* 165:128–138.

753 Van Strien, A., J. Pannekoek, W. Hagemeyer, and T. Verstrael. 2004. A loglinear Poisson  
754 regression method to analyse bird monitoring data. *bird* 482:33–39.

755 Wearn, O. R., and P. Glover-Kapfer. 2019. Snap happy: camera traps are an effective  
756 sampling tool when compared with alternative methods. *Royal Society open*  
757 *science* 6:181748.

758 Yoccoz, N. G., J. D. Nichols, and T. Boulinier. 2001. Monitoring of biological diversity in  
759 space and time. *Trends in ecology & evolution* 16:446–453.

760

761

762 **TABLES**

763

764 Table 1 Summary of the negative-binomial calibration model (NB1) relating SEC  
765 counts to SOCC counts and habitat variables.

Predictor	Estimate	SE	z	p-value
Intercept	1.739	0.104	16.690	<0.001
SOCC (linear)	1.218	0.166	7.343	<0.001
SOCC <sup>2</sup> (quadratic)	-0.370	0.090	-4.125	<0.001
NDVI (15-day mean)	0.266	0.112	2.387	0.017
Habitat area (ha)	-0.034	0.087	-0.388	0.698
SOCC × NDVI	-0.499	0.146	-3.412	<0.001
SOCC <sup>2</sup> × NDVI	0.184	0.063	2.919	0.003

766

767

768

769 **FIGURE CAPTIONS**

770

771 Figure 1. Geographic distribution of transects used in this study across Catalonia. Blue  
772 lines show the 28 specifically designed SOCC transects monitored with both SOCC and  
773 SEC protocols between 2021 and 2025, which were used to calibrate the SOCC–SEC  
774 relationship. Green lines represent all SOCC transects where at least one Common  
775 Quail was detected between 2005 and 2025 ( $N = 205$ ), for which the calibration model  
776 was applied to generate SEC-equivalent abundance-based indicators.

777

778 Figure 2. Mean number of Common Quail males detected per transect ( $\pm$  SD) by the  
779 SOCC and SEC protocols. Only transects with confirmed quail detection were included.  
780 Bars show mean values and error bars indicate standard deviation.

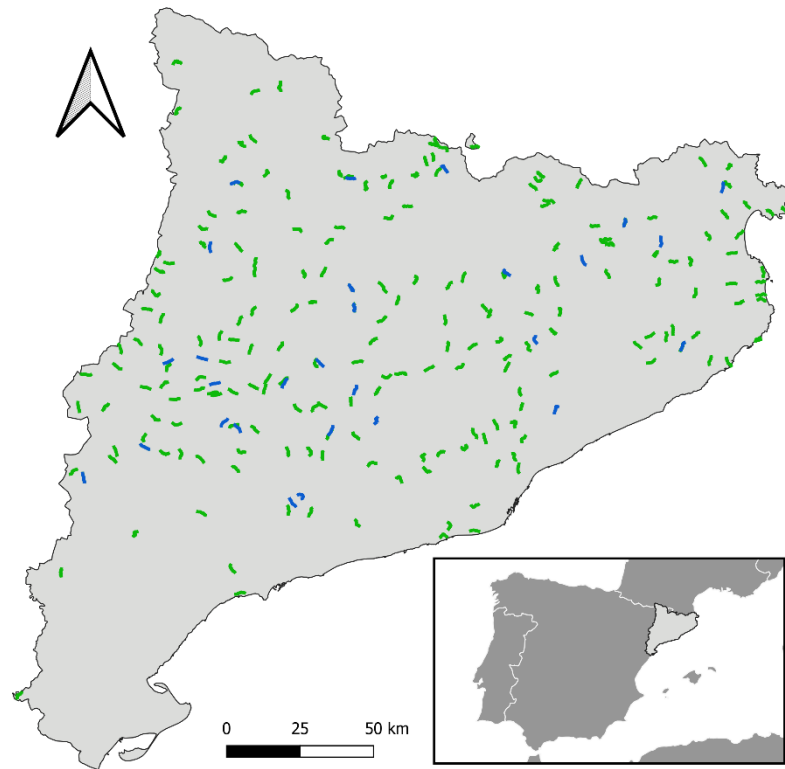
781

782 Figure 3. Predicted SEC-equivalent quail counts as a function of SOCC counts and 15-  
783 day mean NDVI, based on the final NB1 calibration model. The surface illustrates the  
784 combined non-linear effects of SOCC and habitat greenness, as well as their interaction.

785

786 Figure 4 Temporal dynamics of the population index derived from original SOCC  
787 counts (red) and from SEC-equivalent calibrated indicators (blue). Solid lines show  
788 annual TRIM indices and shaded areas represent standard errors. Dashed lines indicate  
789 the fitted log-linear trends, with annual percentage changes shown at the right of each  
790 panel. (A) All transects combined. (B) Transects within high and stable NDVI habitats.  
791 (C) Transects within low or highly variable NDVI habitats. \* denotes a statistically  
792 significant difference between SOCC and SEC-equivalent trends (time  $\times$  series  
793 interaction).

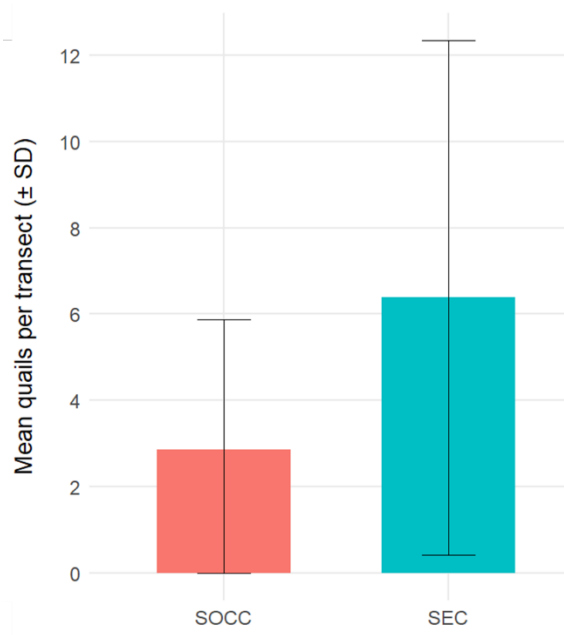
794



795

796 Figure 1

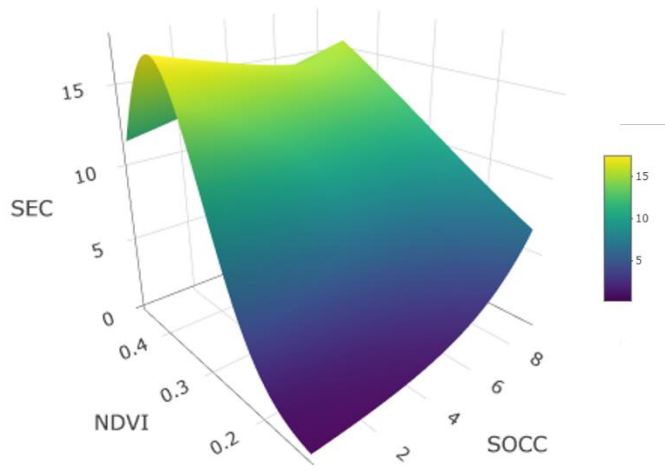
797



798

799 Figure 2

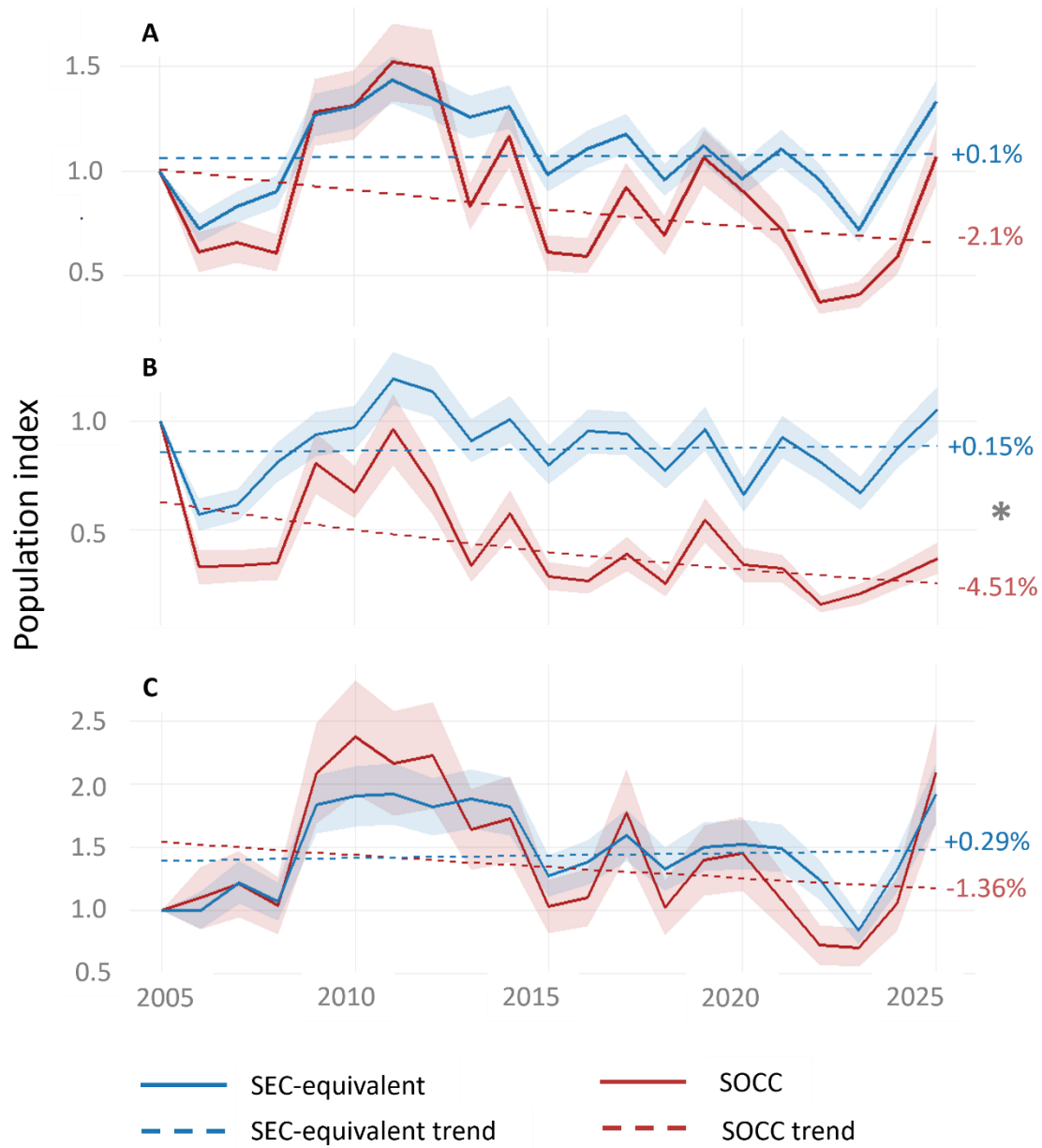
800



801

802 Figure 3

803



804

805 Figure 4

806

807

## Supporting Information S1 – Description of agricultural land-use datasets (SIGPAC and DUN) and habitat categories used in the analyses

To classify suitable agricultural habitats for the Common Quail, we relied on two official, georeferenced land-use datasets that together cover the full study period (2005–2025):

### SIGPAC (2005–2014)

The *Sistema de Información Geográfica de Parcelas Agrícolas* (SIGPAC) is the Spanish Land Parcel Identification System used for the management of the EU Common Agricultural Policy. It provides annual polygon-based information on crop type and agricultural land use at field scale. For the years **2005 to 2014**, suitable quail habitat was identified by selecting all SIGPAC polygons whose *Usa* (“TA”, *Tierra Arable*) and *PS* (“Pastos”) codes corresponded to cereal crops, fallows, herbaceous crops or other dryland habitats consistent with quail breeding ecology.

### DUN (2015–2025)

From 2015 onwards, land-use information was obtained from the *Declaració Única Agraria* (DUN), the annual agricultural declaration system used in Catalonia and derived from SIGPAC. DUN provides detailed crop information at field level and is fully harmonised with CAP reporting requirements. For each year between 2015 and 2025, we selected all DUN polygons corresponding to herbaceous crops, cereals, legumes, fallows and other dryland herbaceous habitats considered suitable for quail breeding.

Table S1 shows the correspondence between SIGPAC and DUN crop codes

### Habitat classification for modelling

All selected SIGPAC and DUN land-use categories were grouped into a single set of suitable breeding habitat types.

These habitat categories were used to:

1. calculate the area of suitable habitat within a 300-m buffer around each transect, and
2. extract vegetation indices (NDVI) for modelling quail abundance and detectability.

Table S1 provides the full lists of categories and their correspondence across datasets.

<b>Sigpac - Suitable habitat for quail</b>	<b>DUN - Suitable habitat for quail (English)</b>	<b>DUN - Suitable habitat for quail (Catalan)</b>
TA Arable Land	Alfalfa	ALFALS
TA Arable Land	Forage mix	BARREJA FARRATGERES
TA Arable Land	Wheat	BLAT
TA Arable Land	Chard	BLEDA
TA Arable Land	Chickpea	CIGRÓ
TA Arable Land	Oat	CIVADA
TA Arable Land	Rapeseed	COLZA
TA Arable Land	Ryegrass	ERB
TA Arable Land	Spelt	ESPELTA
TA Arable Land	Fescue	FESTUCA
TA Arable Land	Sunflower	GIRA-SOL
TA Arable Land	Fallow	GUARET
TA Arable Land	Lentil	LLENTIA
TA Arable Land	Millet	MILL
TA Arable Land	Barley	ORDI
PS Pastures	Pastures < 5 years old	PASTURES DE MENYS DE 5 ANYS
TA Arable Land	Pea	PÈSOL
TA Arable Land	Quinoa	QUINOA
TA Arable Land	Ryegrass	RAIGRAS
TA Arable Land	Rye	SÈGOL
TA Arable Land	Soybean	SOIA
TA Arable Land	Sorghum	SORGO
TA Arable Land	Sainfoin	TREPADELLA
TA Arable Land	Triticale	TRITICALE
TA Arable Land	Vetch	VEÇA

## Supporting Information S2. NDVI-based habitat classification

### S2.1. NDVI data processing

We characterised habitat greenness for all SOCC transects with confirmed Common Quail presence using 15-day NDVI composites derived from Landsat imagery (2005–2025). For each transect and year, we computed:

1. Annual mean NDVI: average NDVI during the breeding season.
2. Intra-annual NDVI variability: standard deviation of NDVI within the breeding season for each year.

These annual summaries were then used to derive three long-term NDVI indicators per transect:

- NDVI\_mean: mean annual NDVI across all sampled years.
- NDVI\_SD\_intra: mean intra-annual NDVI variability.
- NDVI\_SD\_inter: inter-annual variability, measured as the standard deviation of annual NDVI means.
- n\_years: number of years with available NDVI information.

Only transects with confirmed quail detections were retained to ensure ecologically meaningful habitat summarisation.

### S2.2. Clustering analysis

To classify transects according to habitat greenness and stability, we performed k-means clustering ( $k = 2$ ) on the scaled values of the three NDVI indicators:

- NDVI\_mean
- NDVI\_SD\_intra
- NDVI\_SD\_inter

The number of clusters ( $k = 2$ ) was selected to differentiate high-quality stable habitats from low or highly variable habitats, consistent with ecological interpretations from previous NDVI-based analyses of quail occurrence.

Cluster identities were assigned based on maximum NDVI\_mean in the cluster centroids. The two habitat categories were therefore defined as:

- “NDVI high and stable” — high mean NDVI, low variability.
- “NDVI low or highly variable” — low greenness and/or high temporal fluctuation.

### S2.3. Principal Component Analysis (PCA)

To validate the clustering structure, we performed a PCA using the same NDVI indicators. The first two principal components explained 46.2% (PC1) and 33.0% (PC2) of the variance, respectively.

A clear separation between the two NDVI groups was observed along PC1 (Figure S2.2), confirming that the k-means clusters captured meaningful gradients of habitat greenness and stability.

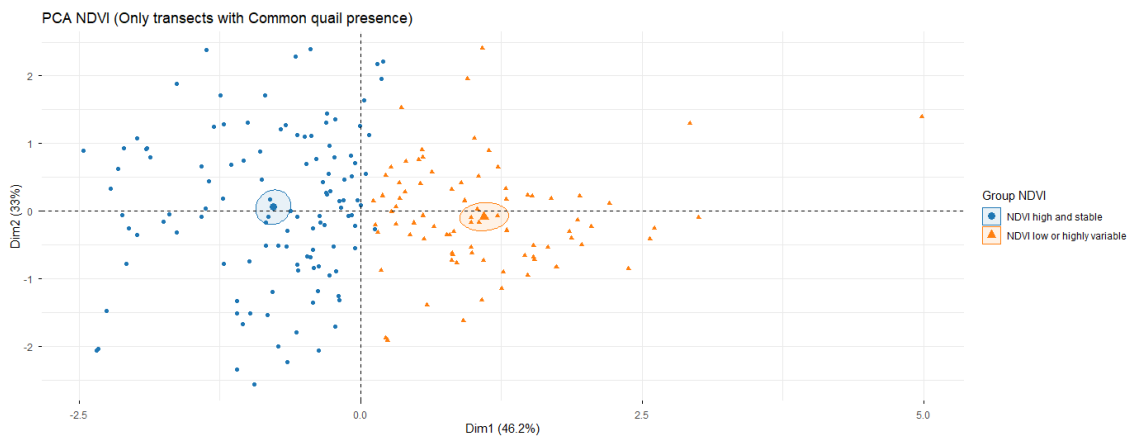


Figure S2.1. *Principal Component Analysis of NDVI indicators.* PCA of NDVI\_mean, NDVI\_SD\_intra and NDVI\_SD\_inter for transects with quail presence. Colours indicate k-means habitat groups, with 95% confidence ellipses. Separation along PC1 validates the clustering structure.

#### S2.4. Statistical comparison of NDVI indicators between groups

To evaluate whether NDVI indicators differed significantly between habitat groups, we performed normality tests (Shapiro–Wilk) and subsequently applied either:

- Student’s t-test (when both groups were normally distributed), or
- Mann–Whitney U test (for non-normal distributions).

The comparison was conducted for (Table S2.1):

- NDVI\_mean
- NDVI\_SD\_intra
- NDVI\_SD\_inter

Table S2.1. Statistical comparison of NDVI indicators between habitat-quality groups. Results of parametric (t-test) and non-parametric (Mann–Whitney U) tests comparing mean NDVI, intra-annual NDVI variability and interannual NDVI variability between the two NDVI-based habitat clusters (“NDVI high and stable” vs. “NDVI low or highly variable”). Reported p-values correspond to two-tailed tests.

Variable	Test	p_value
Mean NDVI	t-test (paramètric)	< 0.001
Intra-annual NDVI SD	NDVI SD Mann–Whitney U (no paramètric)	< 0.001
Interannual NDVI SD	NDVI SD Mann–Whitney U (no paramètric)	< 0.001

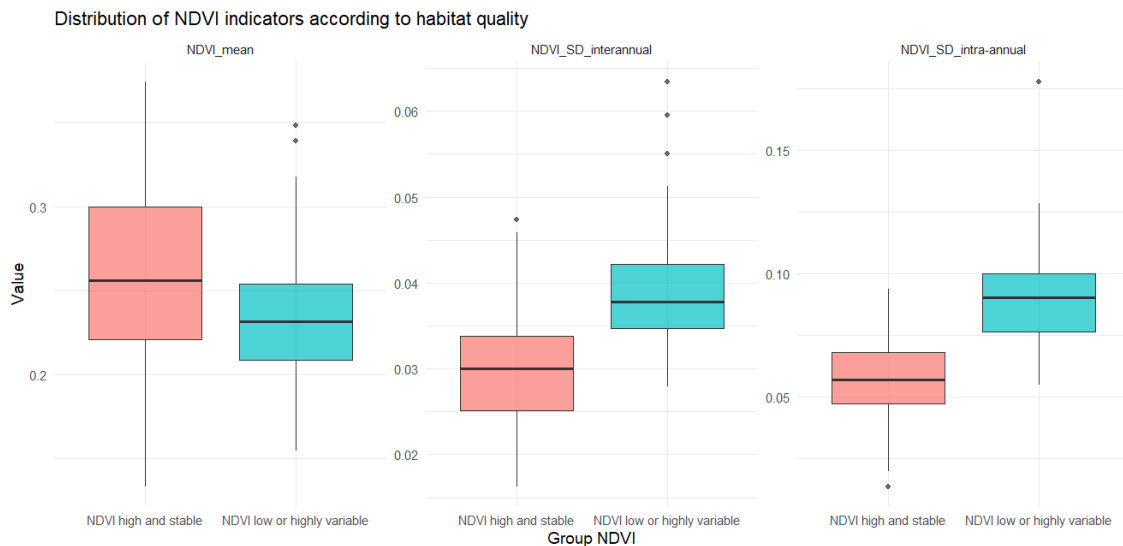


Figure S2.2. *Distribution of NDVI indicators according to habitat-quality group.* Boxplots showing (A) mean NDVI, (B) inter-annual NDVI variability, and (C) intra-annual NDVI variability for the two NDVI groups. High-NDVI stable transects show greater greenness and lower temporal variability.

### Supporting Information S3 – Predictor contribution analysis

Predictor contribution was assessed by refitting reduced models on the exact training dataset used by the final calibration model (n = 58).  $\Delta$ AIC values are expressed relative to the full model specification. The linear SOCC term was the most influential component ( $\Delta$ AIC = 53.5), followed by the quadratic SOCC term ( $\Delta$ AIC = 20.0). NDVI (including its interactions with SOCC) also contributed substantially to model support ( $\Delta$ AIC = 11.9), and removing NDVI interactions alone reduced support by  $\Delta$ AIC = 8.93. Suitable habitat area did not improve model support ( $\Delta$ AIC = -1.85), indicating no detectable contribution of this covariate.

Table S3. Contribution of each predictor to the final calibration model based on AIC differences between the full model and models with individual terms removed.

Removed term	df	AIC	$\Delta$ AIC
Full model	8	282.52	0.00
NDVI_mean + interactions	5	294.45	11.93
socc (linear) + interaction	6	336.02	53.50
socc <sup>2</sup> + interaction	6	302.48	19.96
NDVI interactions only	6	291.45	8.93
Suitable habitat (ha)	7	280.67	-1.85

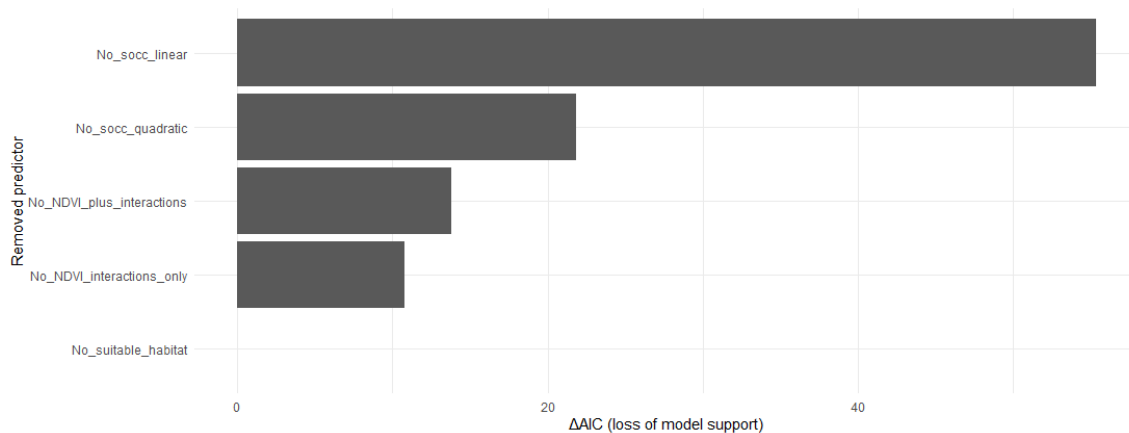


Figure S3.1. Relative importance of each predictor based on  $\Delta$ AIC values obtained by removing individual terms or groups of terms from the full model. Larger  $\Delta$ AIC values indicate greater loss of model support. The linear component of SOCC was the dominant predictor, followed by its quadratic component and NDVI. Suitable habitat area had no detectable influence on model performance.

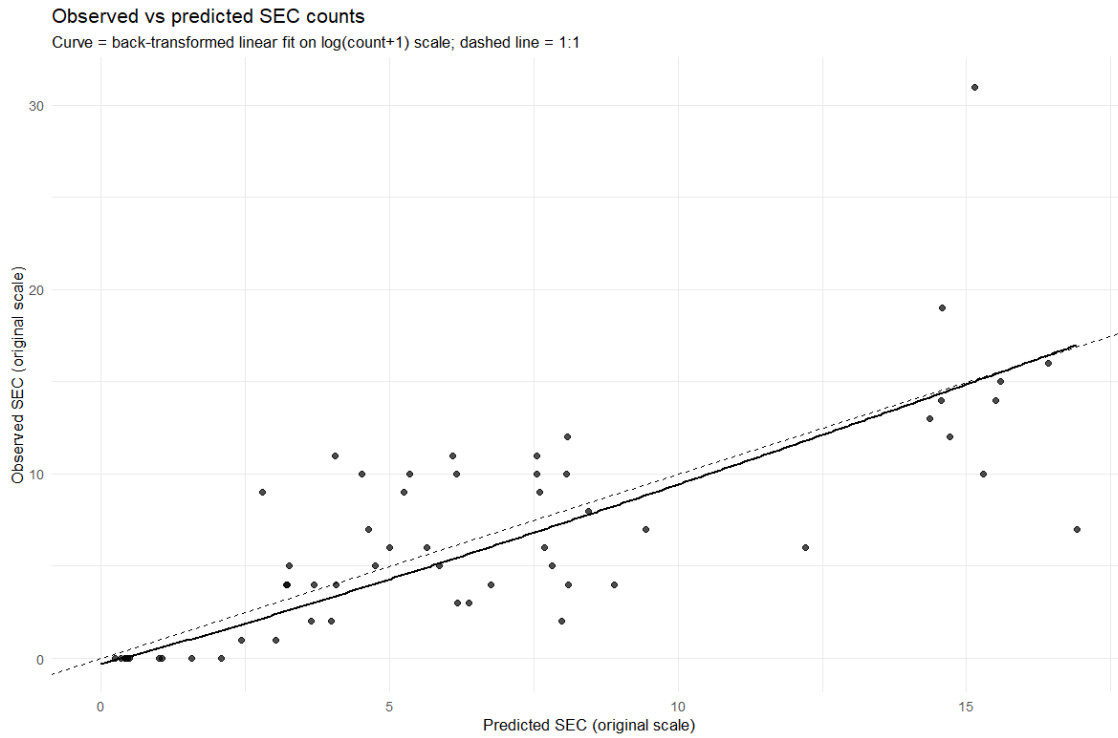


Figure S3.2. Relationship between observed and predicted SEC counts from the final calibration model (negative binomial with log link). Points are shown on the original count scale. The solid curve is the back-transformed fit from a linear regression on  $\log(\text{count}+1)$ , and the dashed line indicates the 1:1 relationship. Pearson correlation was computed on  $\log(\text{count}+1)$  ( $R = 0.87$ ).